The PAF1 complex cell-autonomously promotes oogenesis in *Caenorhabditis elegans*

Short title: PAF1C promotes oogenesis via OMA-1

Yukihiro Kubota[1¶*], Natsumi Ota[2¶], Hisashi Takatsuka[2], Takuma Unno[2], Shuichi Onami[2,3], Asako Sugimoto[4], and Masahiro Ito[1,2]

[1] Department of Bioinformatics, College of Life Sciences, Ritsumeikan University, 1-1-1 Nojihigashi, Kusatsu, Shiga, Japan

[2] Advanced Life Sciences Program, Graduate School of Life Sciences, Ritsumeikan University, 1-1-1 Nojihigashi, Kusatsu, Shiga, Japan

[3]RIKEN Center for Biosystems Dynamics Research, 2-2-3, Minatojima-minamimachi, Chuo-ku, Kobe, Japan

[4] Laboratory of Developmental Dinamics, Graduate School of Life Sciences, Tohoku University, 2-1-1 Katahira, Sendai, Miyagi, Japan

* Corresponding author:

E-mail: yukubota@fc.ritsumei.ac.jp (YK)

¶These authors contribute equally to this work.

Abstract

The RNA polymerase II-associated factor 1 complex (PAF1C) is a protein complex that consists of LEO1, RTF1, PAF1, CDC73, and CTR9, and has been shown to be involved in Pol II-mediated transcriptional and chromatin regulation. Although it has been shown to regulate a variety of biological processes, the precise role of the PAF1C during germ line development has not been clarified. In this study, we found that reduction in the function of the PAF1C components, LEO-1, RTFO-1, PAFO-1, CDC-73, and CTR-9, in *Caenorhabditis elegans* affects cell volume expansion of oocytes. Defects in oogenesis were also confirmed using an oocyte maturation marker, OMA-1::GFP. While four to five OMA-1::GFP-positive oocytes were observed in wild-type animals, their numbers were significantly decreased in *pafo-1* mutant and *leo-1(RNAi)*, *cdc-73(RNAi)*, and *pafo-1(RNAi)* animals. Expression of a functional PAFO-1::mCherry transgene in the germline significantly rescued the oogenesis-defective phenotype of the *pafo-1* mutants, suggesting that expression of the PAF1C in germ cells is required for oogenesis. Notably, overexpression of OMA-1::GFP partially rescued the oogenesis defect in the *pafo-1* mutants. Based on our findings, we propose that the PAF1C promotes oogenesis in a cell-autonomous manner by positively regulating the expression of genes involved in oocyte maturation.

Introduction

During animal development, spatiotemporal regulation of gene transcription is essential for precise regulation of cell behavior. To precisely regulate gene transcription, the recruitment and activation of RNA polymerase II (Pol II) to the transcriptional target

is required. In addition, chromatin remodeling affects DNA accessibility during transcription through epigenetic modification of nucleosomes. The polymerase associated factor 1(PAF1) complex, or PAF1C, is a highly conserved protein complex in eukaryotes, which is involved in multiple aspects of Pol II-mediated transcriptional regulation, including transcriptional elongation, 3′-end processing, and epigenetic modification. Moreover, the PAF1C is involved in the post-transcriptional step of gene expression and translational regulation via its interaction with the regulatory sequences of mRNAs [1, 2].

The PAF1C was originally identified in *Saccharomyces cerevisiae* as an RNA pol II interactor [3-5]. It consists of five subunits (Leo1, Rtf1, Paf1/pancreatic differentiation, Cdc73/parafibromin, and Ctr9) [6, 7]. Although PAF1C is not essential for the viability of *S. cerevisiae*, depletion or mutation of the PAF1 subunits causes severe developmental disorders during the development of somite, neural crest, neuron, heart, and craniofacial cartilage in zebrafish [8-11]. Additionally, the PAF1C affects Notch, Wnt, and Hedgehog signaling [8, 12-14]. The PAF1C has also been reported to regulate the proliferation, differentiation, morphology, cell migration, epidermal morphogenesis, mitophagy, maintenance of stem cells, and tumorigenesis [4, 10, 15-23]. However, the functional importance of the PAF1C in germ cell development has not yet been explored.

The development of the nematode, *Caenorhabditis elegans*, is highly reproducible, which makes it a reliable model organism for analyzing the regulatory mechanism of development. The hermaphrodite gonad of this nematode temporally produces sperm at the late larval stage, which are stored in the spermatheca, and subsequently produces oocytes during the adult stage. During this process, spatiotemporal regulation of gene expression, cell proliferation, cell differentiation, cell shape change, cell growth, and

meiotic progression occurs [24-26]. However, the mechanism of oogenesis has not been fully elucidated.

In this study, we found that all the PAF1C components are involved in promoting the expansion of cell volume of oocytes, and that the expression of OMA-1, a CCCH-type zinc finger protein involved in oocyte maturation, is promoted by the PAF1C in a cell-autonomous manner.

Materials and Methods

C. elegans strains

C. elegans strains used in this study were derived from the wild-type (WT) Bristol strain N2 [27]. Worms were incubated at 20 °C, except those that were fed RNAi bacteria and were maintained at 22 °C.

The *leo-1* locus encodes a predicted polypeptide of 430 amino acids (aa), and the *gk1081* allele (isolated by the *C. elegans* Gene Knockout Consortium) deleted 627 bp that would result in a C-terminally truncated protein of 137 aa (intrinsic 132 aa with an extra 5 aa) [20]. The *rtfo-1* locus encodes a predicted polypeptide of 613 aa, and the *tm5670* allele (isolated by the National Bioresource Project Japan) deleted 361 bp that would result in a C-terminally truncated protein product of 349 aa (intrinsic 314 aa with an extra 35 aa). The *pafo-1* locus encodes a predicted polypeptide of 425 aa, and the *tm13447* allele (isolated by the National Bioresource Project, Japan) deleted 83 bp that would result in a C-terminally truncated protein product of 288 aa (intrinsic 285 aa with an extra 3 aa). The *leo-1(gk1081)* mutant has been shown to produce reduced amounts of C-terminally truncated proteins [20]. The C-terminus of RTF1 in yeast has been shown to be required

for its efficient anchoring to the PAF1C; *rtfo-1(tm5670)* is expected to be a complex formation-defective mutant [28]. We also used the following alleles for construction of mutants: *tjIs57[pie-1p::mCherry::H2B::pie-1 3′-UTR + unc-119(+)]* [29], *bkcSi11[oma-1p::oma-1::GFP::oma-1 3′-UTR, NeoR] IV*, *bkcSi12[pie-1p::pafo-1::mCherry::pie-1 3′-UTR, NeoR]*, *bkcSi13[pie-1p::pafo-1::mCherry::pie-1 3′-UTR, NeoR]* (this work), *tjIs280[pafo-1p::pafo-1::mCherry::pafo-1 3′-UTR, Cbr-unc119(+)]*, *tjIs308[leo-1p::GFP::leo-1::leo-1 3′-UTR, Cbr-unc-119(+)]* [20], *TmC3V[TmIs1230]*, and *TmC5 IV[tmIs1220]* [30].

To obtain *leo-1(gk1081)* homozygote hermaphrodites, *leo-1(gk1081)* was balanced with *TmC5 IV[tmIs1220]*, and Venus-negative homozygote progeny was scored. To obtain *rtfo-1(tm5670) and pafo-1(tm13347)* homozygote hermaphrodites, *rtfo-1(tm5670)* and *pafo-1(tm13347)* were balanced with *TmC3V[TmIs1230]*, and mCherry-negative homozygote progeny was scored.

The strains used in this work are listed in S1 Table.

Plasmid construction

The plasmids used in this study are listed in S2 Table. A miniMos backbone vector, denoted as pYK13, was constructed by inserting a 376 bp fragment containing a multicloning site into a StuI site in pCFJ910. To construct the targeting vectors, the following fragments were amplified and individually subcloned into pYK13 at the NotI and AscI sites. To construct transgenes that expressed GFP-fusion proteins from putative endogenous 5′ -cis regulatory regions of *oma-1*, the genomic fragments, *oma-*

1::GFP derived from the *oma-1* regulatory region (2860 bp), the coding region, and the *oma-1* 3′ -UTR (2935 bp), were PCR amplified and then fused with GFP.

For germ cell-specific expression experiments, the *pafo-1* genome was subcloned into a carboxyl-terminal mCherry-fusion protein expression vector, which has cis regulatory regions of *pie-1*, pYK229, a modified vector derived from pYK13.

Strain construction for rescue experiments

Transgenic worms were prepared by microinjection of the target gene [31]. Strains that expressed *oma-1::GFP* under putative endogenous 5′ -cis regulatory regions and 3′ -cis regulatory region of *oma-1,* and strains that expressed PAFO-1::mCherry under the germ cell-specific regulatory regions of *pie-1* were used for miniMos methods (see below). Single-copy transgenic-insertion worms were generated using the miniMos method [32] for genomic GFP/mCherry-fusion expression and tissue-specific rescue experiments with the wild-type as the host strain. For microinjections, the following mixtures were used: 10 μg/mL each of GFP/mCherry-tagged miniMos-target transgene (*oma-1p::oma-1::GFP:: oma-1 3′-UTR* + *NeoR* plasmid pYK29, *pie-1-1p::pafo-1::mCherry:: pie-1 3′-UTR* + *NeoR* plasmid pYK232); transposase pCFJ601, 50 μg/mL; injection markers *Prab-3::mCherry::unc-54 3′-UTR* plasmid pGH8, 10 μg/mL; *Pmyo-2::mCherry::unc-54 3′-UTR* plasmid pCFJ90, 2.5 μg/mL; *Pmyo-3::mCherry::unc-54 3′-UTR* plasmid pCFJ104, 5 μg/mL; and pBluescript II KS(–), 30 μg/mL; negative selection marker *Phsp-16.41::peel-1::tbb-2 3′-UTR* plasmid pMA122, 10 μg/mL.

The integrated alleles, *tjIs280[pafo-1p::pafo-1::mCherry::pafo-1 3'-UTR*, *Cbr-unc119(+)]*, *bkcSi12[pie-1p::pafo-1::mCherry::pie-1 3'-UTR*, *NeoR]*, and *bkcSi13[pie-1p::pafo-1::mCherry::pie-1 3'-UTR*, *NeoR]* were introduced to the *pafo-1(tm13347)* mutant or *bkcSi11 [oma-1p::oma-1::GFP::oma-1 3'-UTR*, *NeoR]*; *pafo-1(tm13347)* mutant background. Day 1 adult worms were used to score the oogenesis defects.

Feeding RNAi

The worms were fed on RNAi-feeding plates as previously described [33]. Full-length *leo-1*, *rtfo-1*, *pafo-1*, and *cdc-73* cDNAs and 1000 bp *ctr-9* (1st–1000th coding region) cDNA were isolated from a *C. elegans* cDNA library and inserted into the feeding RNAi vector, L4440. An L4440 vector lacking an insert was used as a *control(RNAi)*. After confirming that each inserted sequence was correct, the feeding vectors were individually transformed into *Escherichia coli* HT115 (DE3) samples, which were then seeded separately onto plates of nematode growth medium agar containing Luria-Bertani medium and 50 μg/mL ampicillin, and incubated overnight at 37 °C. Thereafter, each culture was seeded onto a 60 mm feeding agar plate containing 50 μg/mL ampicillin and 1 mM isopropyl *β*-D-1-thiogalactopyranoside and incubated at 23 °C for 2 days. L4-stage worms were transferred to a feeding plate and cultured at 22 °C. Phenotypes of F1 worms were determined at the day 1 adult stage.

Microscopy

Fluorescence and differential interference contrast; DIC microscopy procedures were performed using an Olympus BX63 microscope with an ORCA-Spark camera (Hamamatsu Photonics) and UPlanSApo X60 water NA 1.20 or UPlanXapo X40 NA 0.95 objective lens. The microscope system was controlled using the cellSens Dimension software (Olympus). Images were processed using the ImageJ (NIH) or Adobe Photoshop 2021 software.

Statistical analyses

The *P*-value for the Fisher's exact test for the percentage of animals with oogenesis defects in *leo-1(ok1018)*, *rtfo-1(tm5670)*, and *pafo-1(tm13347)* were calculated for comparison with wild-type animals. The *P*-value for the Fisher's exact test for the percentage of animals with oogenesis defects in *leo-1(RNAi)*, *rtfo-1(RNAi)*, *pafo-1(RNAi)*, *cdc-73(RNAi)*, and *ctr-9(RNAi)* were calculated for comparison with *control(RNAi)* animals. For the OMA-1::GFP overexpression experiment, the *P*-value for the Fisher's exact test for the percentage of animals with oogenesis defects in *pafo-1(tm13347);bkcSi11[oma-1p::oma-1::GFP::oma-1 3'-UTR, NeoR]* was calculated for comparison with *pafo-1(tm13347)* animals.

The *P*-value for the Student's *t*-test of the relative expression level of GFP::LEO-1 at the distal gonad-arm region in *leo-1(RNAi);tjIs308[leo-1p::GFP::leo-1::leo-1 3'-UTR, Cbr-unc-119(+)]* was calculated for comparison with the *control(RNAi);tjIs308[leo-1p::GFP::leo-1::leo-1 3'-UTR, Cbr-unc-119(+)]* animals. The *P*-value for the Student's *t*-test of the relative expression level of PAFO-1::mCherry at the distal gonad-arm region in *pafo-1(RNAi);tjIs280[pafo-1p::pafo-1::mCherry::pafo-1 3'-UTR, Cbr-*

unc119(+)] was calculated for comparison with the *control(RNAi); tjIs280[pafo-1p::pafo-1::mCherry::pafo-1 3'-UTR, Cbr-unc119(+)]* animals. For rescue experiments, the *P*-value for the Student's *t*-test of the number of OMA-1::GFP positive oocytes in *pafo-1(tm13347);tjIs280[pafo-1p::pafo-1::mCherry::pafo-1 3'-UTR];bkcSi11[oma-1p::oma-1::GFP::oma-1 3'-UTR, NeoR], pafo-1(tm13347);bkcSi12[pie-1p::pafo-1::mCherry::pie-1 3'- UTR];bkcSi11[oma-1p::oma-1::GFP::oma-1 3'-UTR, NeoR], pafo-1(tm13347);bkcSi13[pie-1p::pafo-1::mCherry::pie-1 3'- UTR];bkcSi11[oma-1p::oma-1::GFP::oma-1 3'-UTR, NeoR]* were calculated for comparison with the *pafo-1(tm13347);bkcSi11[oma-1p::oma-1::GFP::oma-1 3'-UTR, NeoR]* animals.

Data availability

All data and samples described in this work will be freely provided upon request.

Results

The PAF1C is essential for oogenesis

To analyze whether the PAF1C is involved in germ cell development in *C. elegans*, we observed germ cell development of the posterior gonads in day 1 adults of the PAF1C mutants by DIC microscopy (Fig 1). Compared with the wild-type animals, the cell volume expansion of oocytes was insufficient in the PAF1C mutants, *leo-1(gk1081)*, *rtfo-1(tm5670)*, and *pafo-1(tm13447)* mutants, although the penetrance of *leo-1(gk1081)* was lower than that of the other mutants (Fig 1A–1E and 1P). An integrated transgene, *pafo-1::mCherry*, expressed by the *pafo-1* regulatory element rescued the

oogenesis defect of the *pafo-1(tm13447)* deletion mutant (Fig 1F and 1P). Similar to the observations of deletion mutants, although the penetrance of cell volume expansion defect of the *leo-1(RNAi)* was relatively low, all the five RNAi-knockdown animals of the PAF1C components exhibited cell volume expansion defects (Fig 1G–1M and 1P). The efficiency of both *leo-1(RNAi)* and *pafo-1(RNAi)* was over 90% (Fig. 1N and 1O; S1 Fig; S2 Fig), as measured by the fluorescent signal of GFP::LEO-1 and PAFO-1::mCherry, respectively, at the distal region of the gonad. These results suggest that the PAF1C is essential for oogenesis, and that the contribution of LEO-1 to the PAF1C function may be the lowest among the PAF1C components.

Fig 1. The PAF1C is Essential for Oogenesis.

(A–M) Germ cell development of wild-type (A), *leo-1(gk1018)* (B, C), *rtfo-1(tm5670)* (D), *pafo-1(tm13347)* (E), *pafo-1(tm13347)*, *tjIs280[pafo-1p::pafo-1::mCherry::pafo-1 3'-UTR]* (F), *control(RNAi)* (G), *leo-1(RNAi)* (H, I), *rtfo-1(RNAi)* (J), *pafo-1(RNAi)* (K), *cdc-73(RNAi)* (L), and *ctr-9(RNAi)* (M) in the hermaphrodite day 1 adult posterior gonads. (N, O) Quantitative analysis of the RNAi efficiency of *leo-1(RNAi)* (N) and *pafo-1(RNAi)* (O). *P*-values are indicated for Student's *t*-test in comparison with the *control(RNAi)*. ***$P < 0.005$. The error bars represent ± SD. (P) Percentages of oogenesis defects found in 1 day-adult wild type, mutants, transgenic rescued, *control(RNAi)*, and RNAi-knockdown animals of each PAF1C component. *P*-values are indicated for Fisher's exact test in comparison with WT or *control(RNAi)*. ***$P < 0.005$. Error bars represent ± SD. In all panels, the anterior region of the gonad was to the left, and the dorsal region was at the top of the image. The posterior gonads are shown. The orange dotted lines mark the gonad boundaries. Scale bar (white), 50 μm.

The PAF1C is dispensable for spermatogenesis

Next, we examined whether the PAF1C is involved in spermatogenesis. When nuclei were visualized with mCherry::H2B(histone), sperm-like small cells were detected in wild type and *control(RNAi)* animals. Similarly, sperm-like cells were formed in *pafo-1(tm13447)*, *leo-1(RNAi)*, *pafo-1(RNAi)*, and *cdc-73(RNAi)* animals (Fig 2). Thus, these results suggest that the PAF1C is not essential for spermatogenesis.

Fig 2. The PAF1C is Dispensable for Spermatogenesis.

(A–L) Differential interference contrast (DIC) (A, C, E, G, I, and K) and fluorescence (B, D, F, H, J, and L) images of wild type (A, B), *pafo-1(tm13347)* (C, D), *control(RNAi)* (E, F), *leo-1(RNAi)* (G, H), *pafo-1(RNAi)* (I, J), and *cdc-73(RNAi)* (K, L) day 1 adult animals with *tjIs57[pie-1p::mCherry::H2B::pie-1 3'-UTR]*. In all the panels, the anterior region of the gonad is to the left, and the dorsal region is at the top of the image. The posterior gonads are shown. The orange dotted lines mark the gonad boundaries and the blue dotted lines surround the sperm-like small cells. Scale bar (white), 50 μm.

The PAF1C is involved in the expression of OMA-1 in oocytes

Next, we investigated how the PAF1C regulates oogenesis. To visualize matured oocytes, we used an oocyte maturation marker, OMA-1::GFP, which was derived from the *oma-1* regulatory region (Fig 3A). In the day 1 adult stage of *control(RNAi)* animals, 4.1 OMA-1::GFP-positive cells were arranged linearly in the ventral region of each gonad on an average (N = 15, Fig 3B, 3C, and 3J). In contrast, the average number of OMA-

1::GFP-positive cells were 1.3, 0.27, and 0.13 in *leo-1(RNAi)*, *rtfo-1(RNAi)*, and *pafo-1(RNA)* animals, respectively (N = 15, Fig 3D–3J). These results suggest that the PAF1C positively regulates the expression of OMA-1.

Fig 3. The PAF1C is Essential for the Promotion of Oocyte Maturation.

(A) Genomic structure of the translational GFP-fusion construct of *oma-1*. (B–I) Differential interference contrast (DIC) (B, D, F, and H) and fluorescence (C, E, G, and I) images of *control(RNAi)* (B, C), *leo-1(RNAi)* (D, E), *pafo-1(RNAi)* (F, G), and *cdc-73(RNAi)* (H, I) day 1 adult animals with *bkcSi11[oma-1p::oma-1::GFP::oma-1 3'-UTR]* (C, E, G, and I). (J) Quantification of OMA-1::GFP-positive oocytes. *P*-values are indicated for Student's *t*-test in comparison with *control(RNAi)*. ***$P < 0.005$. The error bars represent ± SD. In all the panels, the anterior region of the gonad is to the left, and the dorsal region is at the top of the image. Posterior gonads are shown. The orange dotted lines mark the gonad boundaries. Asterisk (blue) indicates fertilized egg. Scale bar (white), 50 μm.

Germ cell-specific expression of PAFO-1::mCherry rescues the oocyte maturation-defective phenotype of the *pafo-1(tm13447)* mutant

To determine the tissue in which the expression of PAF1C is required for oocyte maturation, we performed a tissue-specific rescue experiment using the *paflo-1(tm13447)* deletion mutant. In the day 1 adult stage of wild-type animals, approximately 4.7 OMA-1::GFP-positive cells were arranged linearly in the ventral region of each gonad on an

272 average (N = 15, Fig 4B, 4C, and 4L). In contrast, the number of OMA-1::GFP-positive
273 cells was significantly decreased in the *pafo-1(tm13447)* deletion mutant (the average
274 number of OMA-1::GFP-positive cells was 0.6, N = 15; Fig 4D, 4E, and 4L). When, we
275 introduced an integrated *tjIs280[pafo-1::mCherry]* transgene by the *pafo-1* regulatory
276 region (Fig 4A and 4H), it almost completely rescued the oogenesis defect (the average
277 number of OMA-1::GFP-positive cells was 4.5, N = 15, Fig 4F–H and 4L). Similarly,
278 when we introduced integrated *pafo-1::mCherry* transgenes by germ cell-specific
279 regulatory regions of *pie-1*, *bkcSi12* (Fig 4A and 4K), and *bkcSi13* (Fig 4A), they
280 significantly rescued the oogenesis defect of the *pafo-1(tm13447)* deletion mutant (the
281 average number of OMA-1::GFP-positive cells from *pafo-1(tm13447);bkcSi12;bkcSi11*
282 and *pafo-1(tm13447);bkcSi13;bkcSi11* was 2.8 and 3.2, respectively, N = 15, Fig 4I–4L).
283 These results suggest that the PAF1C regulates oogenesis in a cell-autonomous manner.
284 Although the rescue activity with regard to the number of OMA-1::GFP-positive cells
285 was not complete, *bkcSi13[pie-1p::pafo-1::mCherry::pie-1 3'-UTR]* rescued the sterility
286 of the *pafo-1(tm13447)* mutant, and the *pafo-1(tm13447);bkcSi13[pie-1p::pafo-*
287 *1::mCherry::pie-1 3'-UTR]* survived and produced the next generation both in the
288 presence and absence of *bkcSi11[oma-1p::oma-1::GFP::oma-1 3'-UTR]*. Thus, germ cell
289 expression of PAFO-1::mCherry is sufficient for the formation of functional oocytes and
290 its maternal contribution is sufficient for embryonic, larval, larval–adult transition, and
291 germ cell development in the next generation.

292

293 **Fig 4. The PAF1C Promotes Oocyte Maturation in a Cell-autonomous Manner.**

(A) Genomic structures of the translational mCherry-fusion construct of *pafo-1*, germ cell specific mCherry-fusion construct of *pafo-1*, and the deleted region of *pafo-1(tm13447)*. (B–K) Differential interference contrast (DIC) (B, D, F, and I) and fluorescence (C, E, F, G, H, J, and K) images on wild type (B, C), *pafo-1(tm13347)* (D, E), *pafo-1(tm13347);tjIs280[pafo-1p::pafo-1::mCherry::pafo-1 3'-UTR]* (F–H), *pafo-1(tm13347);bkcSi12[pie-1p::pafo-1::mCherry::pie-1 3'-UTR]* (I–K) of day 1 adult animals with *bkcSi11[oma-1p::oma-1:GFP::oma-1 3'-UTR]*. C, E, G, and J indicate the OMA-1::GFP signals from the GFP channel. H and K indicate the *tjIs280*-derived PAFO-1::mCherry signals from the mCherry channel, and the *bkcSi12*-derived PAFO-1-mCherry signals from the mCherry channel, respectively. (L) Quantification of OMA-1::GFP-positive oocytes. *P*-values are indicated for Student's *t*-test in comparison with *pafo-1(tm13347)*. ***$P < 0.005$. The error bars represent ± SD. In all the panels, the anterior region of the gonad is to the left, and the dorsal region is at the top of the image. Posterior gonads are shown. The orange dotted lines mark the gonad boundaries. Asterisk (blue) indicates fertilized egg. Scale bar (white), 50 μm.

Overexpression of OMA-1::GFP partially rescues the oogenesis defect in the *pafo-1(tm13447)* mutant

We tested whether the reduction in the expression of OMA-1 is the major cause of oogenesis defects in the PAF1C mutants. When OMA-1::GFP was overexpressed in the *pafo-1(tm13447)* mutant, the oogenesis defect was partially rescued (Fig 5). Therefore, a possible role of the PAF1C in the germline is to promote oogenesis by positively regulating the expression of *oma-1*.

Fig 5. Overexpression of OMA-1::GFP Partially Rescues the Oogenesis Defect in the *pafo-1(tm13346)* Mutant.

(A, B) Differential interference contrast (DIC) (A) and fluorescence (B) images of *pafo-1(tm13347);bkcSi11[oma-1p::oma-1:GFP::oma-1 3'-UTR]* day 1 adults. (C) Percentages of oogenesis defects found for 1 day-adult wild type, *pafo-1(tm13447)* mutant, and *pafo-1(tm13347);bkcSi11[oma-1p::oma-1:GFP::oma-1 3'-UTR]* animals. *P*-values are indicated for Fisher's exact test in comparison with *pafo-1(tm13347)*. ***$P < 0.005$. In all the panels, the anterior region of the gonad is to the left, and the dorsal region is at the top of the image. Posterior gonad is shown. The orange dotted lines mark the gonad boundaries. Asterisk (blue) indicates fertilized egg. Scale bar (white), 50 μm.

Discussion

The PAF1C is a highly conserved protein complex that consists of five conserved components, LEO1, RTF1, PAF1, CDC73, and CTR9. Although it has been shown to be required in diverse biological processes, its contribution to germ cell development has not yet been explored. In this study, we performed functional analysis of the PAF1C in the germ cell development of *C. elegans* and demonstrate its requirement for cell volume expansion of oocytes and expression of OMA-1 during oogenesis.

Although the PAF1C components, LEO-1 and PAFO-1, are expressed ubiquitously, including in germ cells [20], the PAF1C is required only for oogenesis but not for spermatogenesis. Because the PAF1C is not required for sperm formation, it is unlikely that the oogenesis-defective phenotype is causative of earlier defects in germ cell

development. These results suggest that PAF1C regulates a specific set of genes that are required for oogenesis.

The number of OMA-1::GFP-positive maturing oocytes was decreased in *leo-1(RNAi)*, *rtfo-1(RNAi)*, and *pafo-1(RNAi)* animals and in *pafo-1* deletion mutants. Therefore, one possible role of the PAF1C is the promotion of OMA-1 expression. We also show that the overexpression of OMA-1::GFP partially rescued the oogenesis defect in the *pafo-1* mutant. Therefore, the PAF1C may promote oogenesis by positively regulating the specific set of downstream oocyte maturation regulators, including OMA-1 (Fig 6). Our data also suggest that the germ cell expression of PAF1C is sufficient for the formation of fully functional oocytes and that the maternal contribution of the PAF1C is sufficient for embryonic development, larval development, and larval–adult transition.

It has been shown that *oma-1* and *oma-2* act redundantly to promote the later part of oocyte maturation to complete oocyte maturation [34-36]. In contrast, the cell volume expansion defect of oocytes in the PAF1C-depleted animals and mutants occurred in the early part of the oocyte maturation process. Although the overexpression of OMA-1::GFP partially rescued the cell volume expansion defect of the *pafo-1* mutant, the phenotypic similarity of the oogenesis defect was not observed in the *pafo-1 (tm13447)* mutant and the *oma-1(RNAi);oma-2(RNAi)* animals. These results indicate that the phenotypic severity of PAF1C-depleted animals was stronger than that of OMA-1/2-double depleted animals. Therefore, it is pertinent to discuss as to why the overexpression of OMA-1 rescues the cell volume expansion phenotype of the *pafo-1* mutant. A possible explanation is that although the major function of PAF1C is to promote the expression of OMA-1/2, the PAF1C may also regulate other targets that are involved in the promotion

363 of the cell volume expansion process in parallel with the OMA-1/2 functions. Further
364 analysis is required to confirm this hypothesis.

365 In this study, we found that oogenesis defects were less severe in *leo-1(RNAi)*
366 animals among the animals with RNAi-knockdown of the five components of the PAF1C.
367 Similar to our observations, RTF1, PAF1, CDC73, CTR9, but not LEO1, were reported
368 to be required for the specification of an appropriate number of cardiomyocytes and for
369 elongation of the heart tube in zebrafish [10]. Taken together, these observations suggest
370 that in the specific context of the differentiation process, among the five PAF1C
371 components, the requirement for LEO-1 is less critical, and this difference is conserved
372 in vertebrates and invertebrates. At of date, there are several possible avenues for
373 exploring this phenomenon. In yeast, Ctr9, Cdc73, and Rtf1, but not Leo1, were shown
374 to require PAF1 at normal levels, and loss of Cdc73 resulted in a lower abundance of
375 RTf1 [7, 37]. Therefore, it is expected that the other four components may achieve only
376 a part of the PAF1C function in the absence of LEO-1. Although all the PAF1C
377 components are required for its function, each component has a specific role in regulating
378 the expression of gene encoding cell differentiation regulators, possibly by affecting the
379 formation of the protein complex, specific protein–protein interactions, and protein–
380 DNA/RNA interactions. Further studies are required to determine how PAF1C regulates
381 tissue-specific development in multicellular organisms.

382

383 **Fig 6. Models for the PAF1C-dependent Regulation of Cell Volume Expansion of**
384 **Oocytes.**

385 (A) The PAF1C and RNA polymerase II (RNA pol II) are recruited to the regulatory

386 region of target genes, and directly or indirectly promote the expression of the oocyte
387 maturation regulators. (B) During oocyte maturation, the PAF1C promotes oocyte
388 maturation regulators, which then promote cell volume expansion in the ventral region of
389 the gonad.

390

391 Conclusion

392 In summary, we propose that the PAF1C promotes oogenesis in a cell-autonomous
393 manner by positively regulating the oocyte maturation regulators, including OMA-1.

394

395 Acknowledgements

396 We would like to thank Dr. Eisuke Sumiyoshi for his help with the initial phase of
397 observation of the phenotype. We also thank Mr. Arashi Ezaki and Mr. Tasuku Hamazaki
398 for their helpful comments. Some strains were provided by the CGC, which is funded by
399 the NIH Office of Research Infrastructure Programs (grant number P40 OD010440),
400 the *C. elegans* Gene Knockout Consortium, and the National Bioresource Project in Japan
401 (led by S. Mitani).

402

403

404 References

405 1. Jaehning JA. The Paf1 complex: platform or player in RNA polymerase II
406 transcription? Biochimica et biophysica acta. 2010;1799(5-6):379-88. Epub 2010/01/12. doi:
407 10.1016/j.bbagrm.2010.01.001. PubMed PMID: 20060942; PubMed Central PMCID:
408 PMCPMC2862274.
409 2. Francette AM, Tripplehorn SA, Arndt KM. The Paf1 Complex: A Keystone of

Nuclear Regulation Operating at the Interface of Transcription and Chromatin. Journal of molecular biology. 2021;433(14):166979. Epub 2021/04/04. doi: 10.1016/j.jmb.2021.166979. PubMed PMID: 33811920; PubMed Central PMCID: PMCPMC8184591.

3. Shi X, Chang M, Wolf AJ, Chang CH, Frazer-Abel AA, Wade PA, et al. Cdc73p and Paf1p are found in a novel RNA polymerase II-containing complex distinct from the Srbp-containing holoenzyme. Molecular and cellular biology. 1997;17(3):1160-9. Epub 1997/03/01. doi: 10.1128/mcb.17.3.1160. PubMed PMID: 9032243; PubMed Central PMCID: PMCPMC231841.

4. Shi X, Finkelstein A, Wolf AJ, Wade PA, Burton ZF, Jaehning JA. Paf1p, an RNA polymerase II-associated factor in Saccharomyces cerevisiae, may have both positive and negative roles in transcription. Molecular and cellular biology. 1996;16(2):669-76. Epub 1996/02/01. doi: 10.1128/mcb.16.2.669. PubMed PMID: 8552095; PubMed Central PMCID: PMCPMC231046.

5. Wade PA, Werel W, Fentzke RC, Thompson NE, Leykam JF, Burgess RR, et al. A novel collection of accessory factors associated with yeast RNA polymerase II. Protein expression and purification. 1996;8(1):85-90. Epub 1996/08/01. doi: 10.1006/prep.1996.0077. PubMed PMID: 8812838.

6. Mueller CL, Jaehning JA. Ctr9, Rtf1, and Leo1 are components of the Paf1/RNA polymerase II complex. Molecular and cellular biology. 2002;22(7):1971-80. Epub 2002/03/09. doi: 10.1128/mcb.22.7.1971-1980.2002. PubMed PMID: 11884586; PubMed Central PMCID: PMCPMC133696.

7. Mueller CL, Porter SE, Hoffman MG, Jaehning JA. The Paf1 complex has functions independent of actively transcribing RNA polymerase II. Molecular cell. 2004;14(4):447-56. Epub 2004/05/20. doi: 10.1016/s1097-2765(04)00257-6. PubMed PMID: 15149594.

8. Akanuma T, Koshida S, Kawamura A, Kishimoto Y, Takada S. Paf1 complex homologues are required for Notch-regulated transcription during somite segmentation. EMBO reports. 2007;8(9):858-63. Epub 2007/08/28. doi: 10.1038/sj.embor.7401045. PubMed PMID: 17721442; PubMed Central PMCID: PMCPMC1973952.

9. Nguyen CT, Langenbacher A, Hsieh M, Chen JN. The PAF1 complex component Leo1 is essential for cardiac and neural crest development in zebrafish. Developmental biology. 2010;341(1):167-75. Epub 2010/02/25. doi: 10.1016/j.ydbio.2010.02.020. PubMed PMID: 20178782; PubMed Central PMCID: PMCPMC2854236.

10. Langenbacher AD, Nguyen CT, Cavanaugh AM, Huang J, Lu F, Chen JN. The PAF1 complex differentially regulates cardiomyocyte specification. Developmental biology. 2011;353(1):19-28. Epub 2011/02/23. doi: 10.1016/j.ydbio.2011.02.011. PubMed PMID: 21338598; PubMed Central PMCID: PMCPMC3075326.

11. Jurynec MJ, Bai X, Bisgrove BW, Jackson H, Nechiporuk A, Palu RAS, et al. The Paf1 complex and P-TEFb have reciprocal and antagonist roles in maintaining multipotent neural crest progenitors. Development (Cambridge, England). 2019;146(24). Epub 2019/12/01. doi: 10.1242/dev.180133. PubMed PMID: 31784460; PubMed Central PMCID: PMCPMC6955205.

12. Mosimann C, Hausmann G, Basler K. Parafibromin/Hyrax activates Wnt/Wg target gene transcription by direct association with beta-catenin/Armadillo. Cell. 2006;125(2):327-41. Epub 2006/04/25. doi: 10.1016/j.cell.2006.01.053. PubMed PMID: 16630820.

13. Mosimann C, Hausmann G, Basler K. The role of Parafibromin/Hyrax as a nuclear Gli/Ci-interacting protein in Hedgehog target gene control. Mechanisms of development. 2009;126(5-6):394-405. Epub 2009/04/17. doi: 10.1016/j.mod.2009.02.002. PubMed PMID: 19368795.

14. Tenney K, Gerber M, Ilvarsonn A, Schneider J, Gause M, Dorsett D, et al. Drosophila Rtf1 functions in histone methylation, gene expression, and Notch signaling. Proceedings of the National Academy of Sciences of the United States of America. 2006;103(32):11970-4. Epub 2006/08/03. doi: 10.1073/pnas.0603620103. PubMed PMID: 16882721; PubMed Central PMCID: PMCPMC1567682.

15. Lin L, Zhang JH, Panicker LM, Simonds WF. The parafibromin tumor suppressor protein inhibits cell proliferation by repression of the c-myc proto-oncogene. Proceedings of the National Academy of Sciences of the United States of America. 2008;105(45):17420-5. Epub 2008/11/07. doi: 10.1073/pnas.0710725105. PubMed PMID: 18987311; PubMed Central PMCID: PMCPMC2582266.

16. Moniaux N, Nemos C, Schmied BM, Chauhan SC, Deb S, Morikane K, et al. The human homologue of the RNA polymerase II-associated factor 1 (hPaf1), localized on the 19q13 amplicon, is associated with tumorigenesis. Oncogene. 2006;25(23):3247-57. Epub 2006/02/24. doi: 10.1038/sj.onc.1209353. PubMed PMID: 16491129.

17. Ponnusamy MP, Deb S, Dey P, Chakraborty S, Rachagani S, Senapati S, et al. RNA polymerase II associated factor 1/PD2 maintains self-renewal by its interaction with Oct3/4 in mouse embryonic stem cells. Stem cells (Dayton, Ohio). 2009;27(12):3001-11. Epub 2009/10/13. doi: 10.1002/stem.237. PubMed PMID: 19821493; PubMed Central PMCID: PMCPMC2891238.

18. Zhang K, Haversat JM, Mager J. CTR9/PAF1c regulates molecular lineage identity, histone H3K36 trimethylation and genomic imprinting during preimplantation development. Developmental biology. 2013;383(1):15-27. Epub 2013/09/17. doi: 10.1016/j.ydbio.2013.09.005. PubMed PMID: 24036311; PubMed Central PMCID: PMCPMC4903072.

19. Zheng L, Shu WJ, Li YM, Mari M, Yan C, Wang D, et al. The Paf1 complex

transcriptionally regulates the mitochondrial-anchored protein Atg32 leading to activation of mitophagy. Autophagy. 2020;16(8):1366-79. Epub 2019/09/17. doi: 10.1080/15548627.2019.1668228. PubMed PMID: 31525119; PubMed Central PMCID: PMCPMC7469518.

20. Kubota Y, Tsuyama K, Takabayashi Y, Haruta N, Maruyama R, Iida N, et al. The PAF1 complex is involved in embryonic epidermal morphogenesis in Caenorhabditis elegans. Developmental biology. 2014;391(1):43-53. Epub 2014/04/12. doi: 10.1016/j.ydbio.2014.04.002. PubMed PMID: 24721716.

21. Bai X, Kim J, Yang Z, Jurynec MJ, Akie TE, Lee J, et al. TIF1gamma controls erythroid cell fate by regulating transcription elongation. Cell. 2010;142(1):133-43. Epub 2010/07/07. doi: 10.1016/j.cell.2010.05.028. PubMed PMID: 20603019; PubMed Central PMCID: PMCPMC3072682.

22. Carpten JD, Robbins CM, Villablanca A, Forsberg L, Presciuttini S, Bailey-Wilson J, et al. HRPT2, encoding parafibromin, is mutated in hyperparathyroidism-jaw tumor syndrome. Nature genetics. 2002;32(4):676-80. Epub 2002/11/16. doi: 10.1038/ng1048. PubMed PMID: 12434154.

23. Ding L, Paszkowski-Rogacz M, Nitzsche A, Slabicki MM, Heninger AK, de Vries I, et al. A genome-scale RNAi screen for Oct4 modulators defines a role of the Paf1 complex for embryonic stem cell identity. Cell stem cell. 2009;4(5):403-15. Epub 2009/04/07. doi: 10.1016/j.stem.2009.03.009. PubMed PMID: 19345177.

24. Arur S. Signaling-Mediated Regulation of Meiotic Prophase I and Transition During Oogenesis. Results and problems in cell differentiation. 2017;59:101-23. Epub 2017/03/02. doi: 10.1007/978-3-319-44820-6_4. PubMed PMID: 28247047; PubMed Central PMCID: PMCPMC5436704.

25. Huelgas-Morales G, Greenstein D. Control of oocyte meiotic maturation in C. elegans. Seminars in cell & developmental biology. 2018;84:90-9. Epub 2017/12/16. doi: 10.1016/j.semcdb.2017.12.005. PubMed PMID: 29242146; PubMed Central PMCID: PMCPMC6019635.

26. Kim S, Spike C, Greenstein D. Control of oocyte growth and meiotic maturation in Caenorhabditis elegans. Advances in experimental medicine and biology. 2013;757:277-320. Epub 2012/08/09. doi: 10.1007/978-1-4614-4015-4_10. PubMed PMID: 22872481; PubMed Central PMCID: PMCPMC3819423.

27. Brenner S. The genetics of Caenorhabditis elegans. Genetics. 1974;77(1):71-94. Epub 1974/05/01. PubMed PMID: 4366476; PubMed Central PMCID: PMCPMC1213120.

28. Warner MH, Roinick KL, Arndt KM. Rtf1 is a multifunctional component of the Paf1 complex that regulates gene expression by directing cotranscriptional histone

518 modification. Molecular and cellular biology. 2007;27(17):6103-15. Epub 2007/06/20. doi:
519 10.1128/mcb.00772-07. PubMed PMID: 17576814; PubMed Central PMCID:
520 PMCPMC1952162.
521 29. Toya M, Terasawa M, Nagata K, Iida Y, Sugimoto A. A kinase-independent role for
522 Aurora A in the assembly of mitotic spindle microtubules in Caenorhabditis elegans embryos.
523 Nature cell biology. 2011;13(6):708-14. Epub 2011/05/17. doi: 10.1038/ncb2242. PubMed
524 PMID: 21572421.
525 30. Dejima K, Hori S, Iwata S, Suehiro Y, Yoshina S, Motohashi T, et al. An Aneuploidy-
526 Free and Structurally Defined Balancer Chromosome Toolkit for Caenorhabditis elegans.
527 Cell reports. 2018;22(1):232-41. Epub 2018/01/04. doi: 10.1016/j.celrep.2017.12.024. PubMed
528 PMID: 29298424.
529 31. Mello CC, Kramer JM, Stinchcomb D, Ambros V. Efficient gene transfer in
530 C.elegans: extrachromosomal maintenance and integration of transforming sequences. The
531 EMBO journal. 1991;10(12):3959-70. Epub 1991/12/01. PubMed PMID: 1935914; PubMed
532 Central PMCID: PMCPMC453137.
533 32. Frokjaer-Jensen C, Davis MW, Sarov M, Taylor J, Flibotte S, LaBella M, et al.
534 Random and targeted transgene insertion in Caenorhabditis elegans using a modified Mos1
535 transposon. Nature methods. 2014;11(5):529-34. Epub 2014/05/14. doi: 10.1038/nmeth.2889.
536 PubMed PMID: 24820376; PubMed Central PMCID: PMCPMC4126194.
537 33. Kamath RS, Martinez-Campos M, Zipperlen P, Fraser AG, Ahringer J.
538 Effectiveness of specific RNA-mediated interference through ingested double-stranded RNA
539 in Caenorhabditis elegans. Genome biology. 2001;2(1):Research0002. Epub 2001/02/24. doi:
540 10.1186/gb-2000-2-1-research0002. PubMed PMID: 11178279; PubMed Central PMCID:
541 PMCPMC17598.
542 34. Detwiler MR, Reuben M, Li X, Rogers E, Lin R. Two zinc finger proteins, OMA-1
543 and OMA-2, are redundantly required for oocyte maturation in C. elegans. Developmental
544 cell. 2001;1(2):187-99. Epub 2001/11/13. doi: 10.1016/s1534-5807(01)00026-0. PubMed PMID:
545 11702779.
546 35. Tsukamoto T, Gearhart MD, Spike CA, Huelgas-Morales G, Mews M, Boag PR, et
547 al. LIN-41 and OMA Ribonucleoprotein Complexes Mediate a Translational Repression-to-
548 Activation Switch Controlling Oocyte Meiotic Maturation and the Oocyte-to-Embryo
549 Transition in Caenorhabditis elegans. Genetics. 2017;206(4):2007-39. Epub 2017/06/04. doi:
550 10.1534/genetics.117.203174. PubMed PMID: 28576864; PubMed Central PMCID:
551 PMCPMC5560804.
552 36. Spike CA, Coetzee D, Eichten C, Wang X, Hansen D, Greenstein D. The TRIM-NHL
553 protein LIN-41 and the OMA RNA-binding proteins antagonistically control the prophase-to-

554 metaphase transition and growth of Caenorhabditis elegans oocytes. Genetics.
555 2014;198(4):1535-58. Epub 2014/09/28. doi: 10.1534/genetics.114.168831. PubMed PMID:
556 25261698; PubMed Central PMCID: PMCPMC4256770.
557 37. Squazzo SL, Costa PJ, Lindstrom DL, Kumer KE, Simic R, Jennings JL, et al. The
558 Paf1 complex physically and functionally associates with transcription elongation factors in
559 vivo. The EMBO journal. 2002;21(7):1764-74. Epub 2002/04/03. doi: 10.1093/emboj/21.7.1764.
560 PubMed PMID: 11927560; PubMed Central PMCID: PMCPMC125365.
561

562

563 Supporting information

564 **S1 Fig. Analysis of the Efficiency of RNAi Knockdown of *leo-1*.**

565 **S2 Fig. Analysis of the Efficiency of RNAi Knockdown of *pafo-1*.**

566 **S1 Table. *Caenorhabditis elegans* Strains Constructed for this Study.**

567 **S2 Table. Plasmids Constructed for this Study.**
568

569

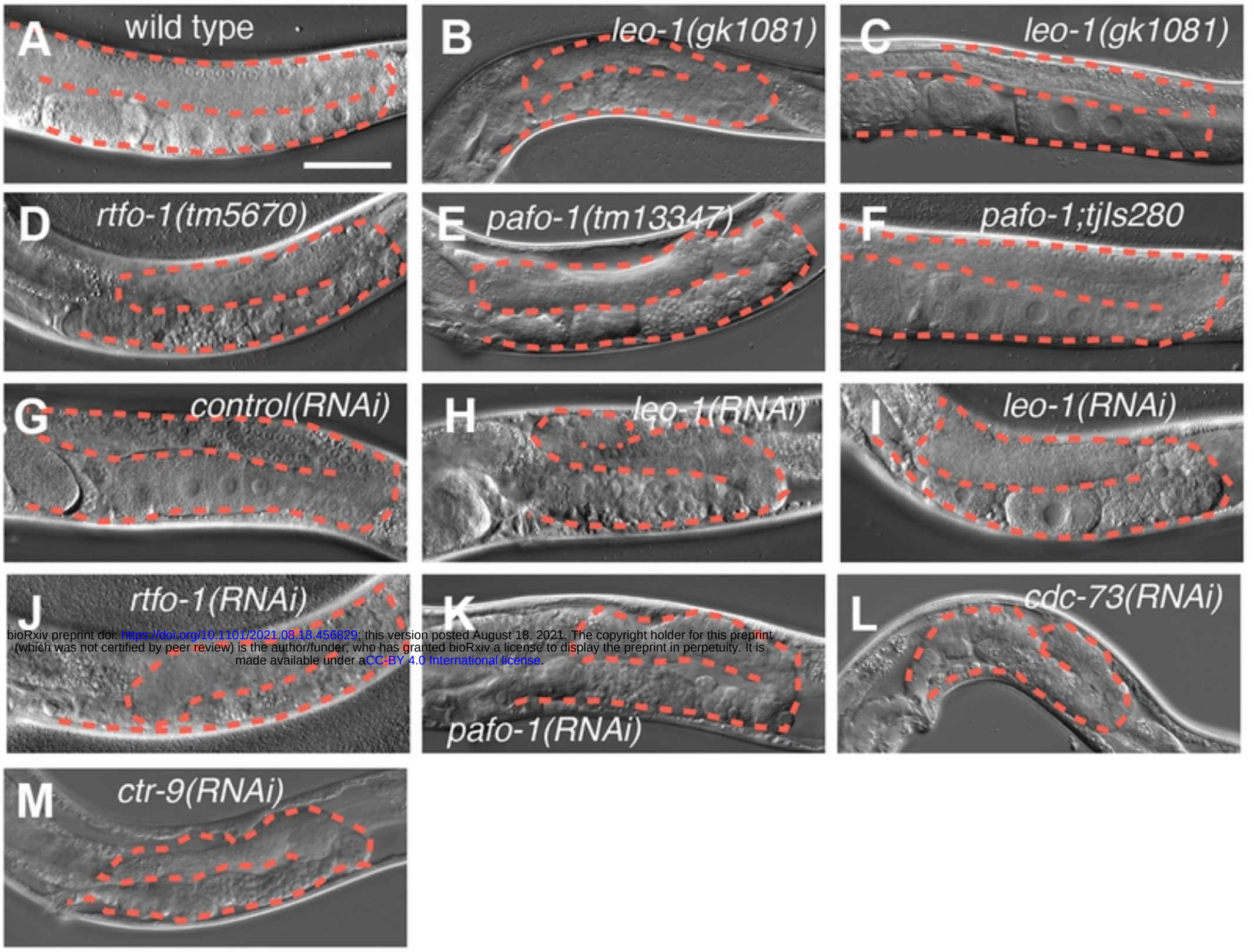

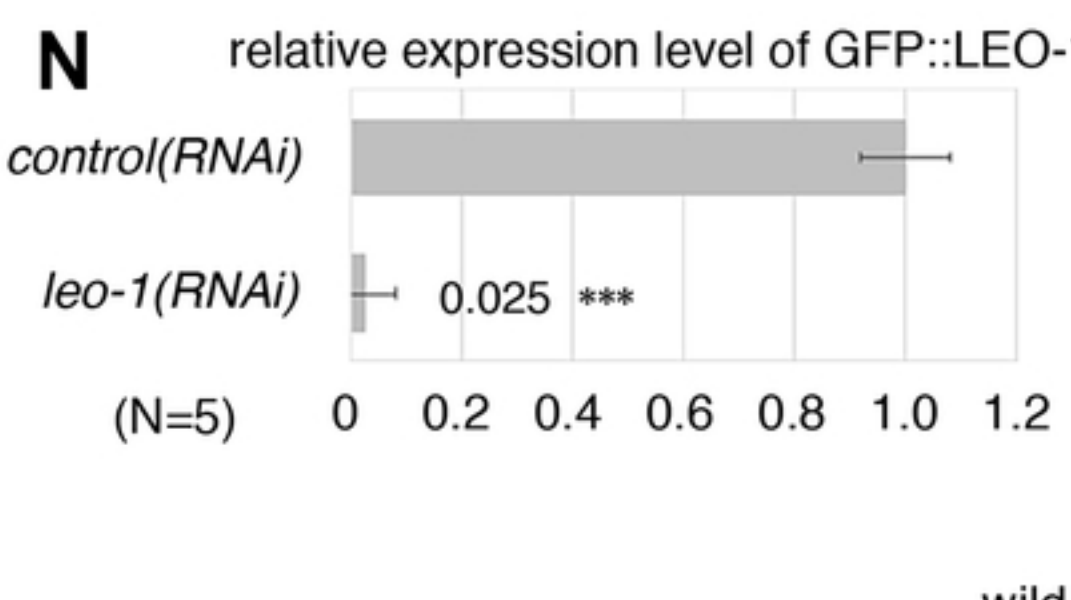

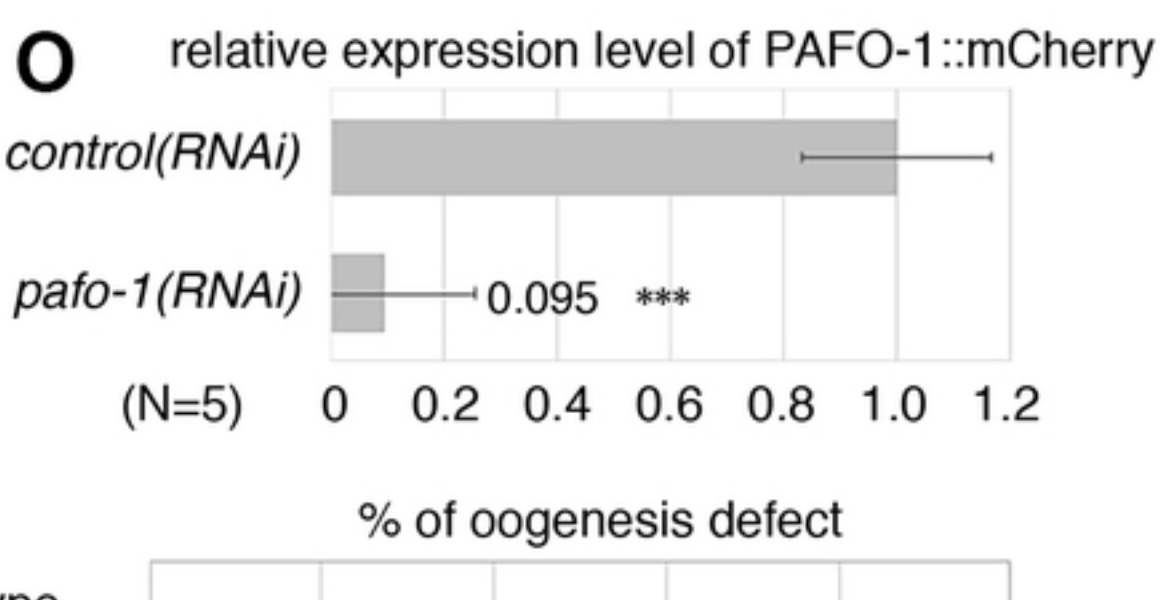

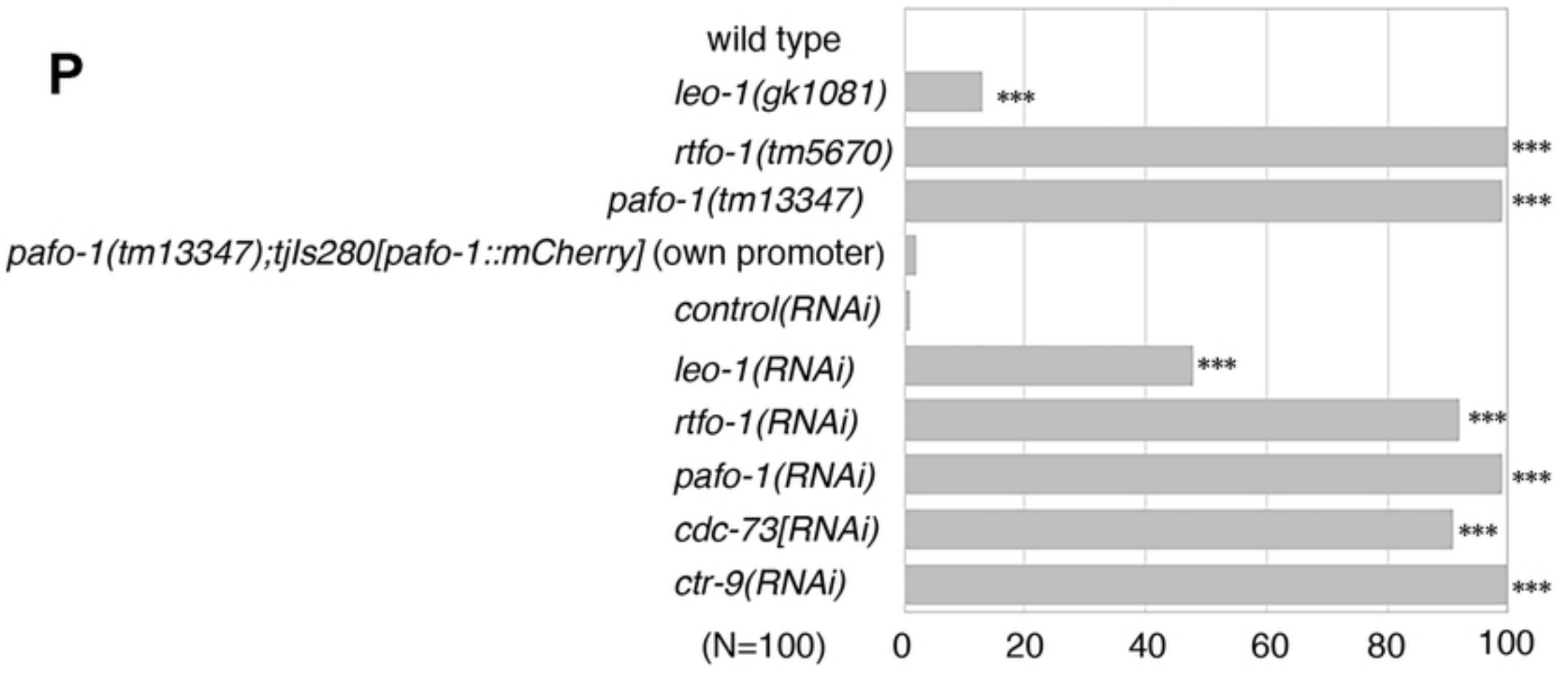

Figure 1

DIC

mCherry::H2B(histone)

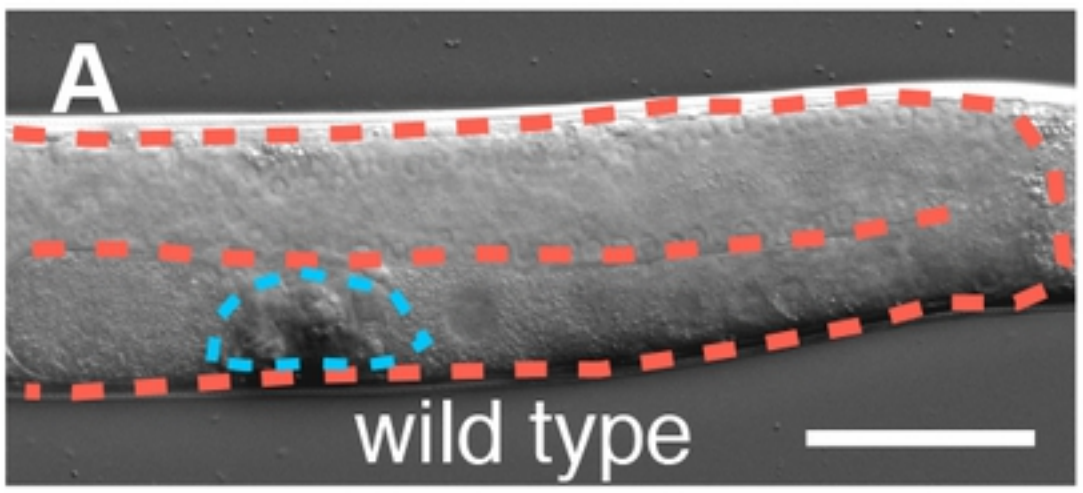

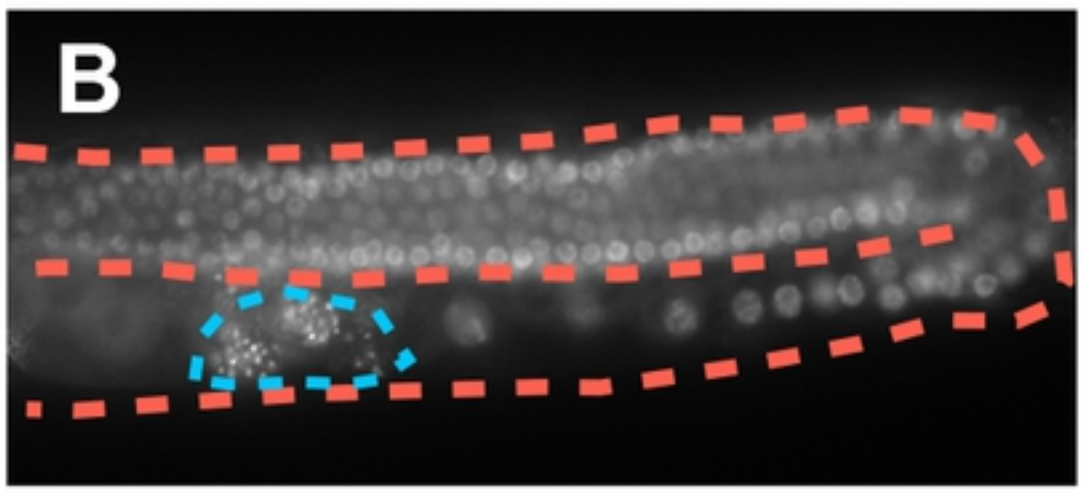

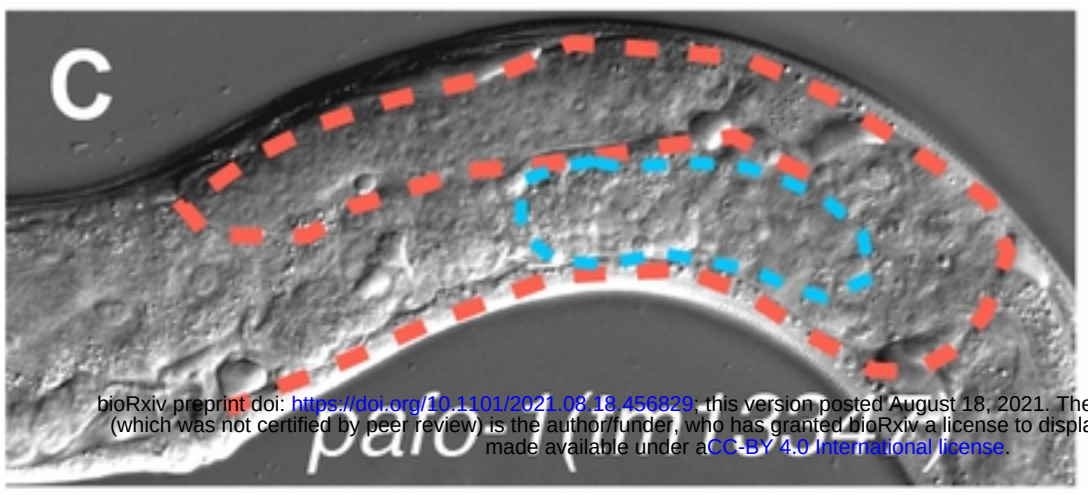

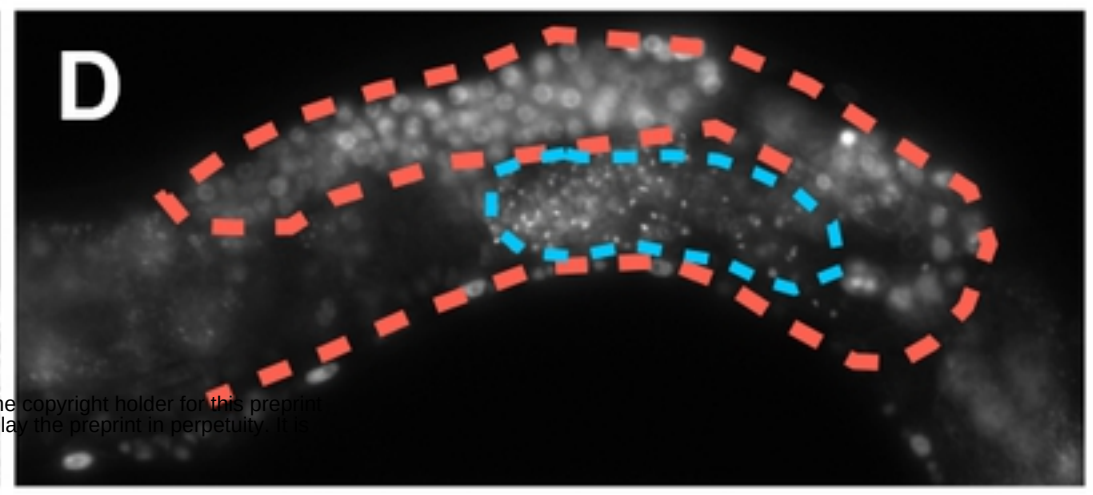

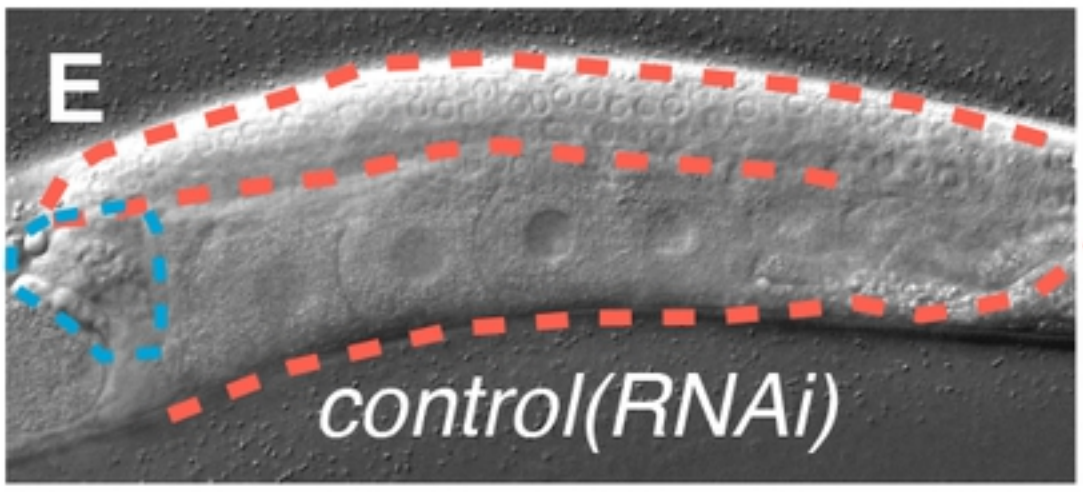

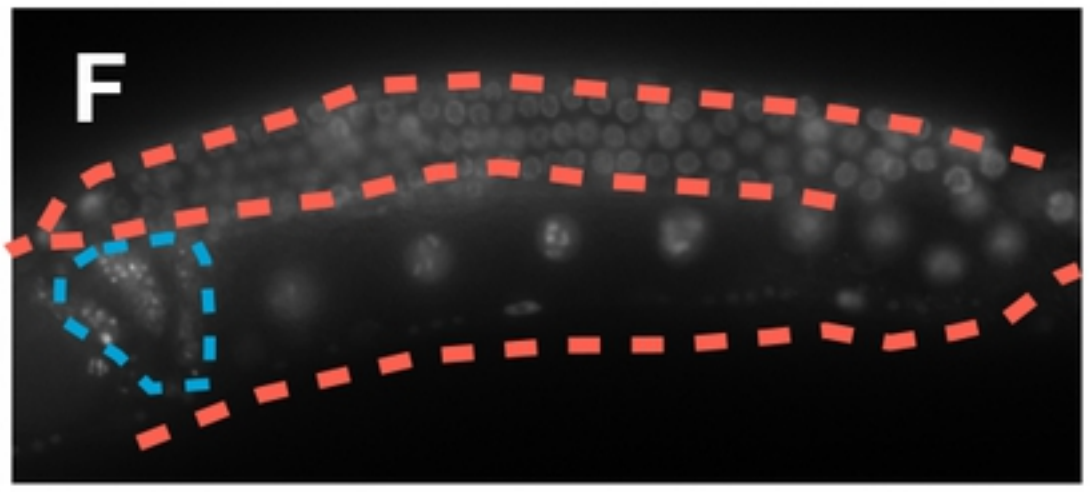

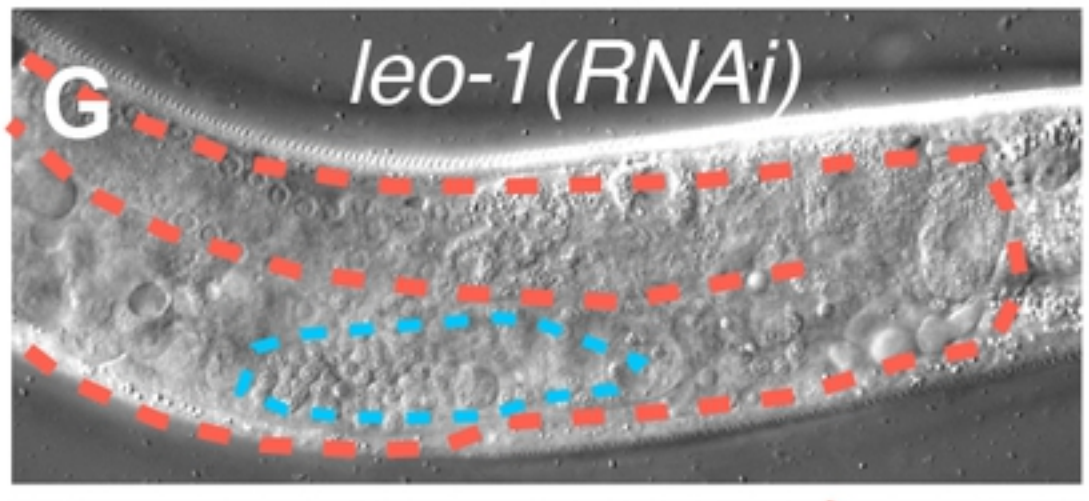

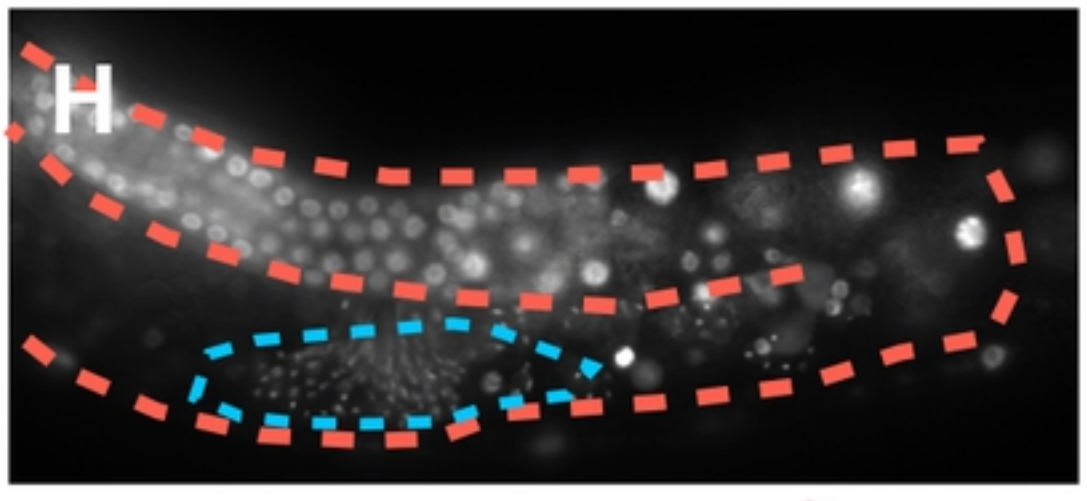

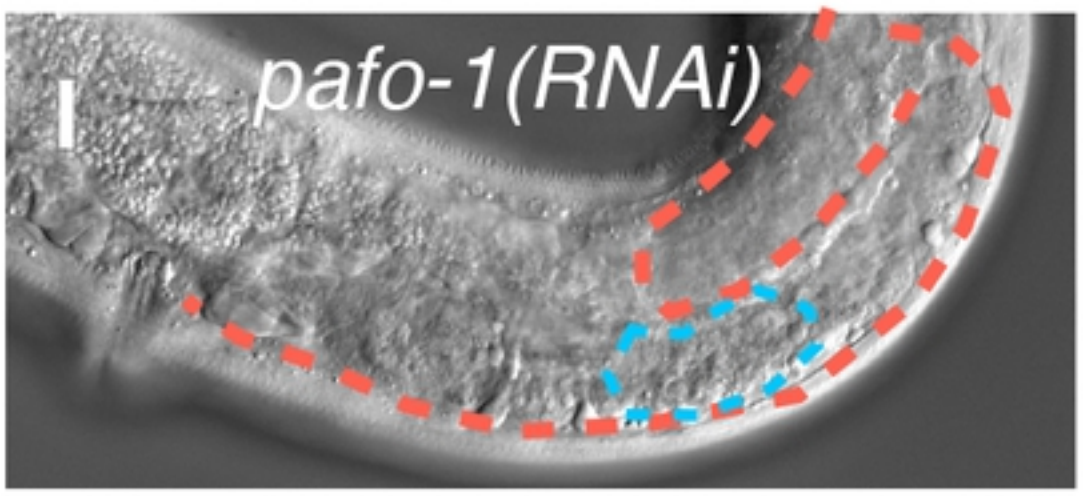

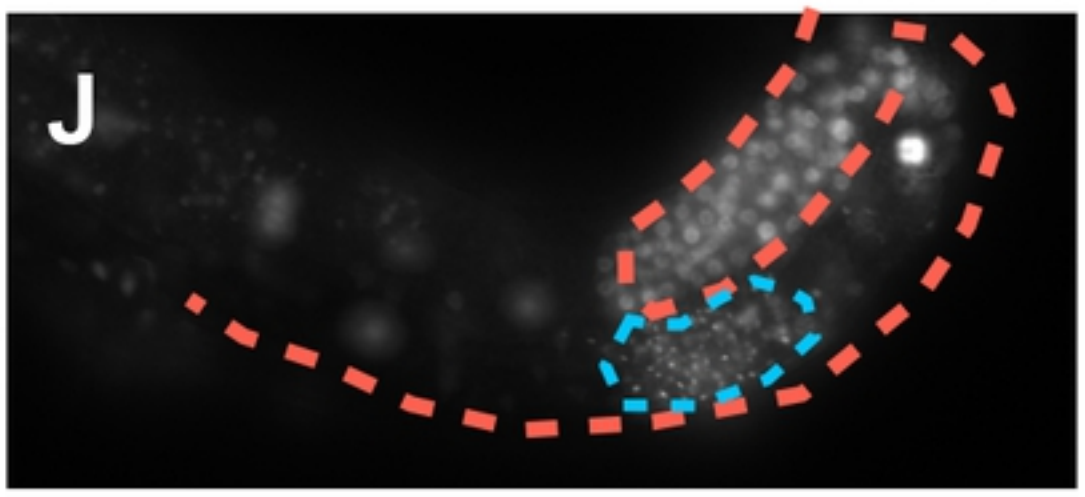

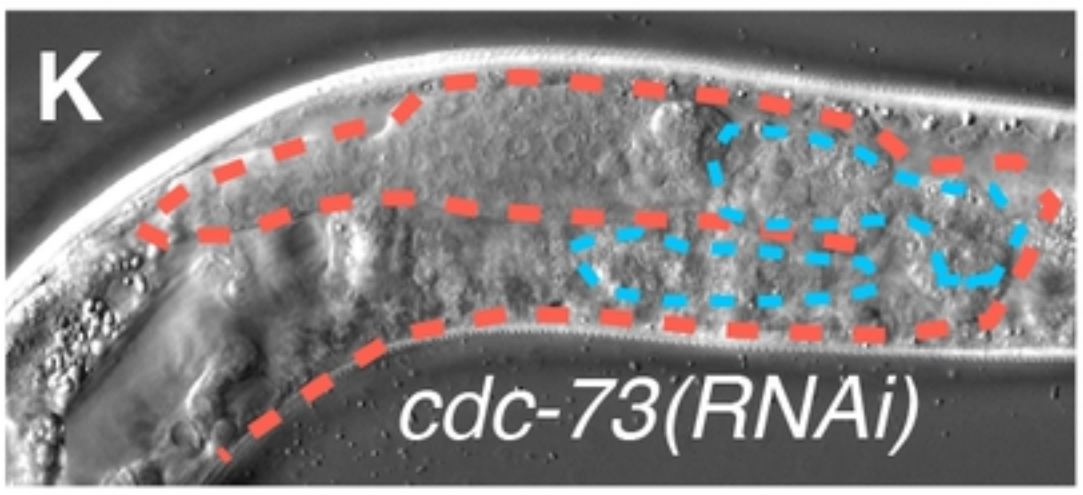

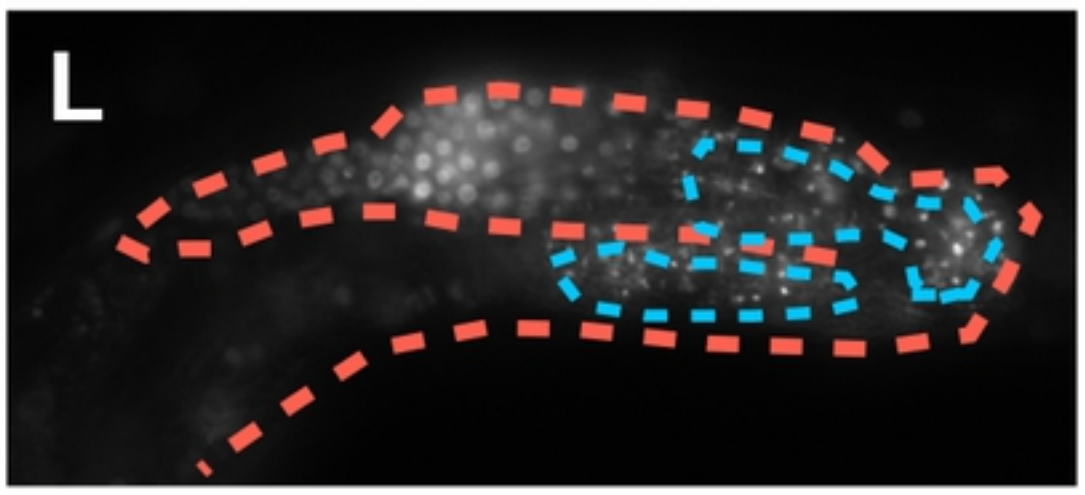

Figure 2

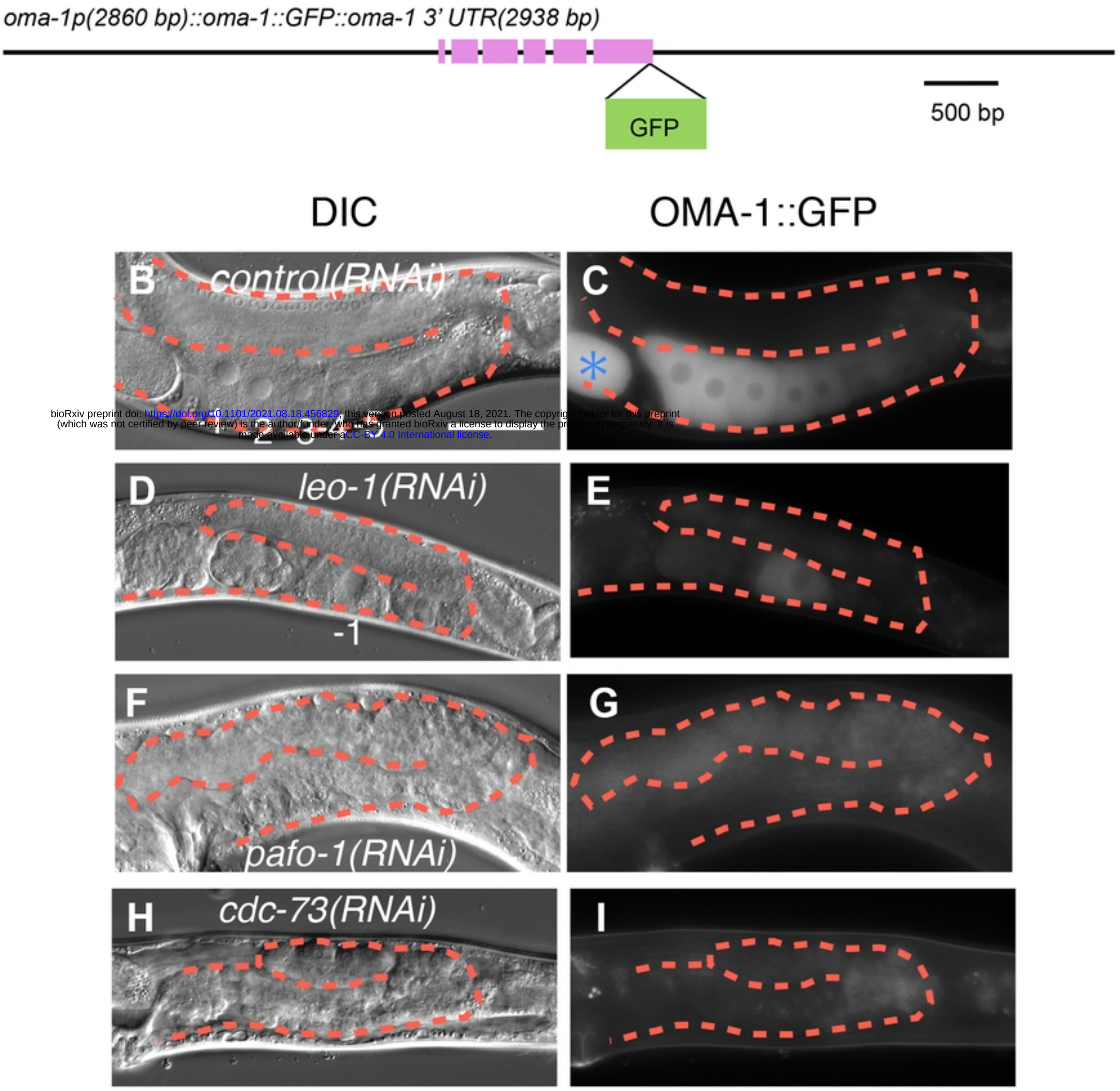

Figure 3

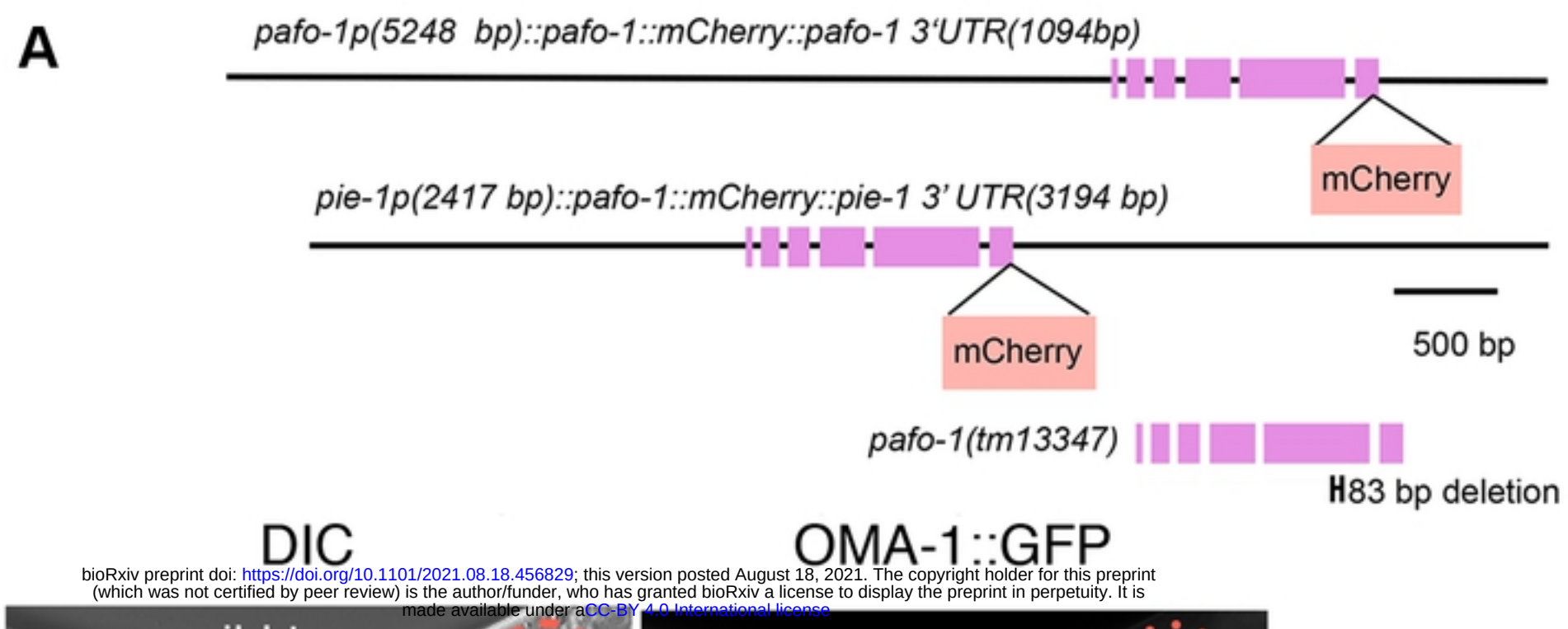

Figure 4

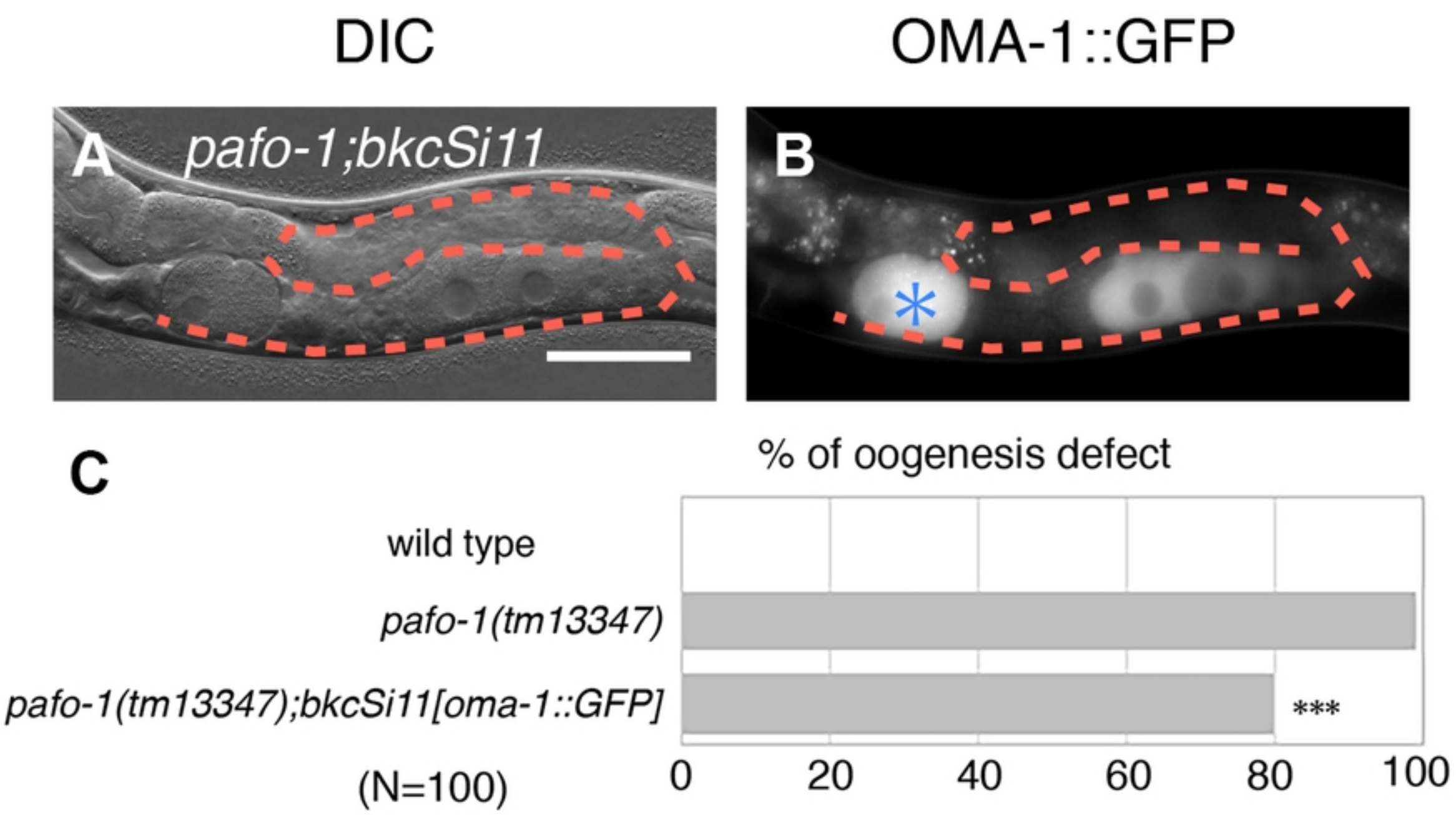
DIC
OMA-1::GFP
A
pafo-1;bkcSi11
B
C
% of oogenesis defect
wild type
pafo-1(tm13347)
pafo-1(tm13347);bkcSi11[oma-1::GFP]
***
(N=100)
0
20
40
60
80
100

Figure 5

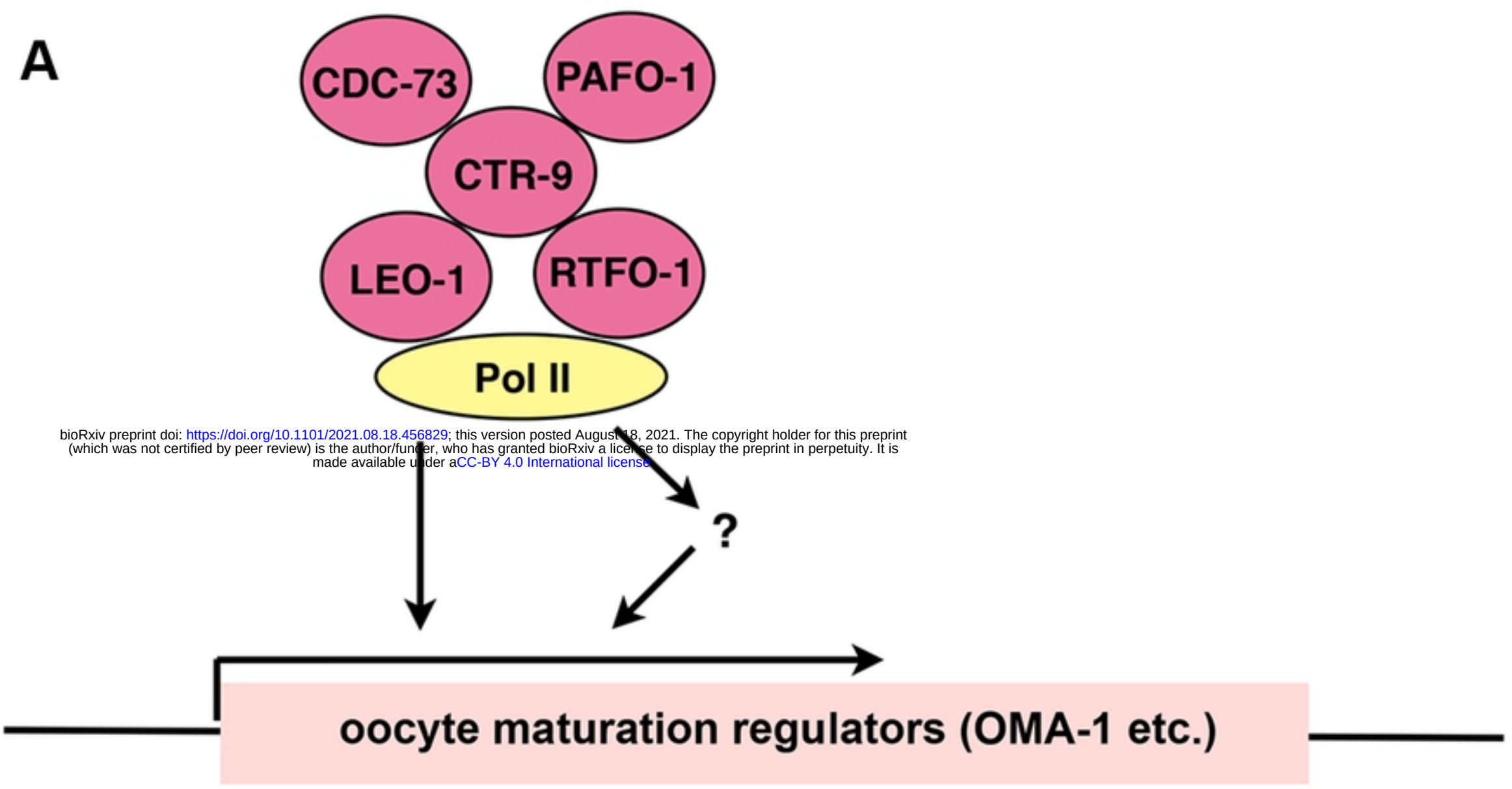

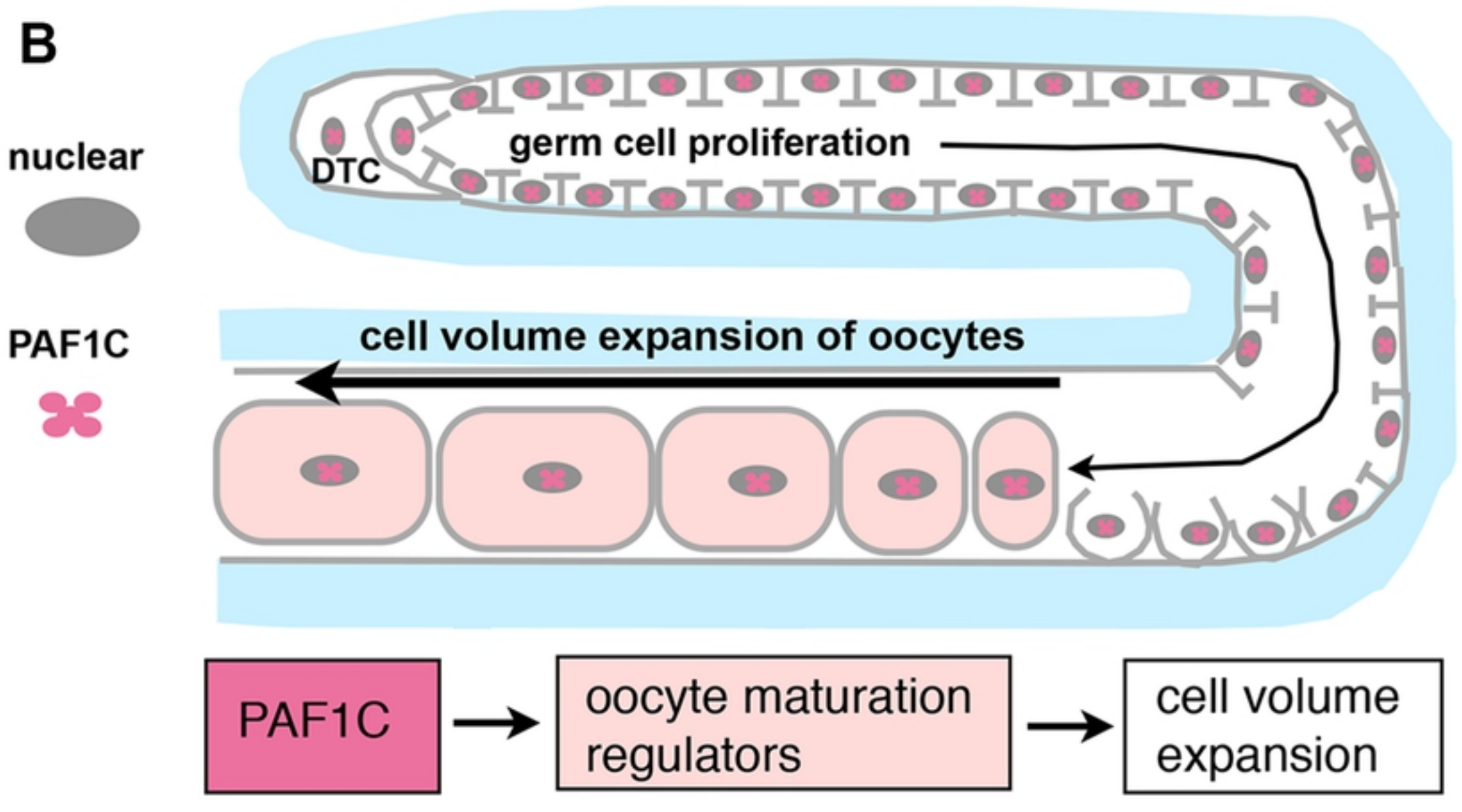

Figure 6

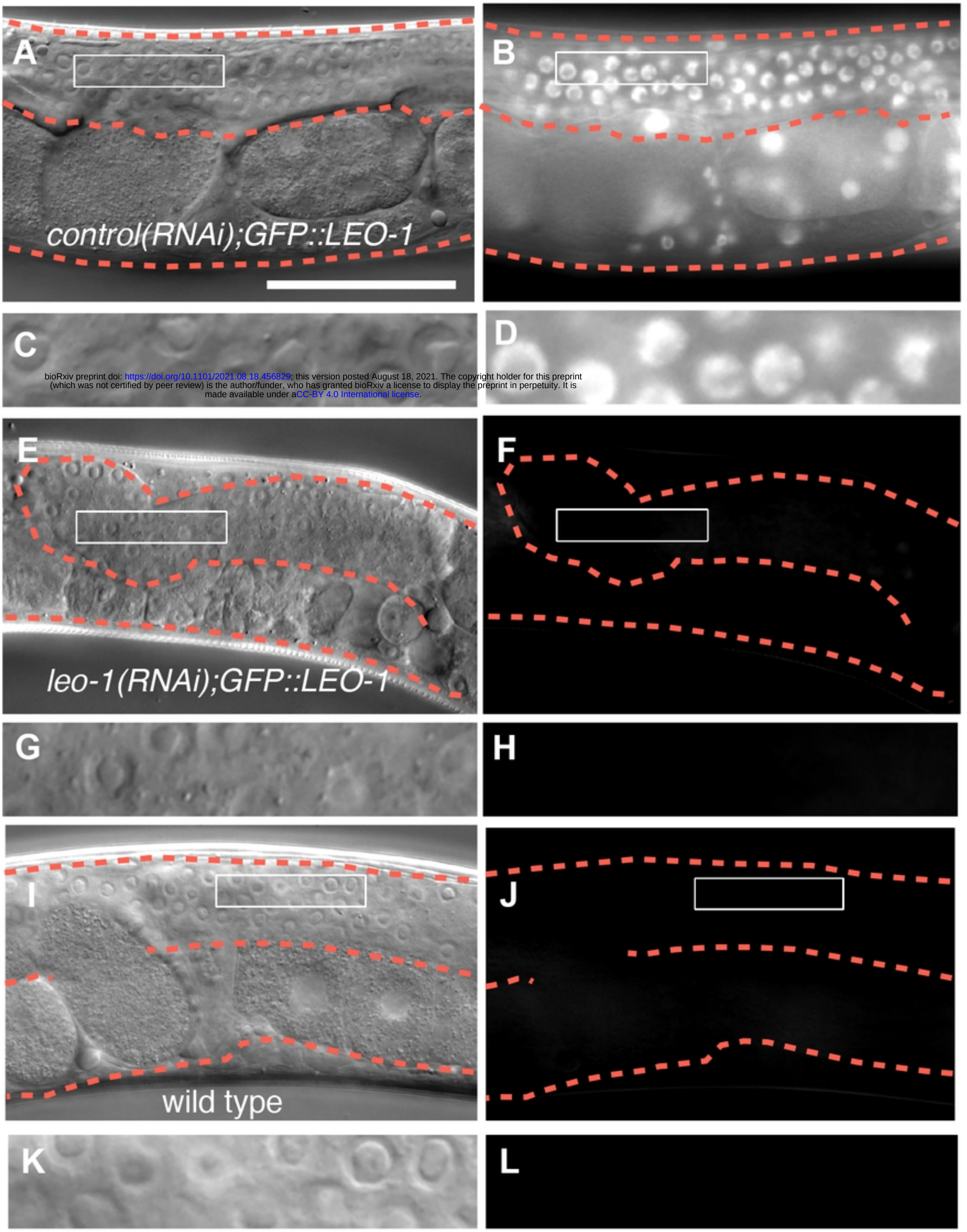

Figure S1

Figure S2